More Experiments on Color Images

Anonymous Authors

March 2024

Abstract

Thank you for your valuable comments and suggestions! According to your advice, we have conducted more experiments on CBSD68.

1 Loss functions

The loss function for a k-strictly pseudo-contractive denoiser is

$$\mathbb{E}\| \mathrm{D}_\sigma(x+\xi_\sigma;\theta) - x\|_1 + r\max\{\|kI+(1-k)J\|_*, 1-\epsilon\}. \tag{1}$$

The loss function for a pseudo-contractive denoiser is

$$\mathbb{E}\| \mathrm{D}_\sigma(x+\xi_\sigma;\theta) - x\|_1 + r\max\{\|(S-2I)^{-1}S\|_*, 1-\epsilon\}, \tag{2}$$

where $x \sim p$, $\sigma \sim U[\sigma_{\min}, \sigma_{\max}], \xi_\sigma \sim \mathcal{N}(0, \sigma^2)$.

2 Denoising Performance

We learn pseudo-contractive denoiser (PC-DRUNet) and k-strictly pseudo-contractive denoiser (SPC-DRUNet) with $k = \frac{1}{2}$. We use CBSD68 as a test set to show the effectiveness of our method. For a fair comparison, all denoisers are trained with DIV2K, and the patch sizes are set to 64. The PSNR values are given in Table 1 on CBSD68.

It can be seen from Table 1 that, compared with MMO, NE-DRUNet, and Prox-DRUNet, the proposed SPC-DRUNet and PC-DRUNet achieves higher PSNR values. Compared with the unconstrained DRUNet, PC-DRUNet shows only 0.01dB performance decrease.

3 Assumption validations

In the experiments, the strictly pseudo-contractive and pseudo-contractive conditions are softly constrained by the loss functions (1) and (2) with a trade-off parameter r. We validate the conditions in Table 2. Please note that, the norms given in Table 2 is a maximum w.r.t. the evaluation point. To give more clarity,

Table 1: Average denoising PSNR performance of different denoisers on CBSD68 dataset, for various noise levels σ.

σ	15	25	40
FFDNet	33.86	31.18	28.81
DnCNN	33.88	31.20	28.89
DRUNet	**34.14**	**31.54**	**29.33**
MMO	32.74	30.20	28.25
NE-DRUNet	32.97	30.54	28.50
Prox-DRUNet	33.18	30.60	28.38
SPC-DRUNet	34.12	31.51	29.32
PC-DRUNet	**34.14**	**31.53**	**29.32**

when evaluating the $\|J\|_*$ of DRUNet with $\sigma = 15$ for CBSD68, Gaussian noise with $\sigma = 15$ is added to each image in CBSD68. This process produces multiple norm values, and the largest value 9.544, as shown in Table 2, is considered the maximization value of the norms at different evaluation points since only the biggest value matters. It is important to note that validating a denoiser as non-expansive requires it to be non-expansive at every point.

As shown in Table 2, DRUNet without spectral regularization term is neither non-expansive nor pseudo-contractive. When PC-DRUNet and SPC-DRUNet are trained by the loss functions (1) and (2) with $r = 10^{-3}$, the norms $\|\frac{1}{2}I+\frac{1}{2}J\|_*$ and $\|(S-2I)^{-1}S\|_*$ are smaller than 1. It validates the effectiveness of the proposed training strategy.

Table 2: Maximal values of different norms on CBSD68 dataset for various noise levels σ.

σ	15	25	40	Max. Norm
DRUNet	9.544	10.81	13.16	$\|J\|_*$
DRUNet	1.614	2.998	1.775	$\|\frac{1}{2}I+\frac{1}{2}J\|_*$
DRUNet	4.364	4.429	4.346	$\|(S-2I)^{-1}S\|_*$
SPC-DRUNet ($r = 10^{-3}$)	0.995	0.991	0.999	$\|\frac{1}{2}I+\frac{1}{2}J\|_*$
SPC-DRUNet ($r = 10^{-4}$)	1.014	1.186	1.440	$\|\frac{1}{2}I+\frac{1}{2}J\|_*$
PC-DRUNet ($r = 10^{-3}$)	0.988	0.999	0.996	$\|(S-2I)^{-1}S\|_*$
PC-DRUNet ($r = 10^{-4}$)	1.020	1.001	1.246	$\|(S-2I)^{-1}S\|_*$

4 Deblurring

In Table 3, we give average deblurring PSNR and SSIM values on CBSD68. It can be seen that compared with other convergent PnP methods, the proposed PnPI-HQS shows 1.11dB and 0.78dB improvement in PSNR with $\sigma = 12.75$ and $\sigma = 17.85$ respectively. For a detailed PSNR and SSIM values on each kernel, see Tables 4-5.

Table 3: Average deblurring PSNR and SSIM performance by different methods on CBSD68 dataset with Levin's 8 kernels with $\sigma = 12.75$ and 17.85.

	$\sigma = 12.75$		$\sigma = 12.75$	
	PSNR	SSIM	PSNR	SSIM
MMO-FBS	26.35	0.7100	25.72	0.7000
NE-PGD	26.58	0.7277	25.94	0.6983
Prox-DRS	26.64	0.7200	25.99	0.6900
DPIR	27.65	0.7738	26.75	0.7293
PnPI-GD	26.41	0.6962	25.61	0.6633
PnPI-HQS	**27.75**	**0.7797**	**26.77**	**0.7386**
PnPI-FBS	26.83	0.7451	25.97	0.7081

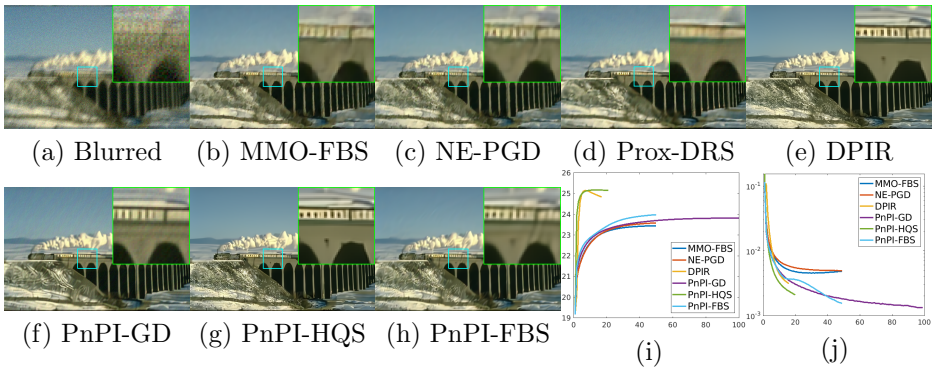

(a) Blurred (b) MMO-FBS (c) NE-PGD (d) Prox-DRS (e) DPIR

(f) PnPI-GD (g) PnPI-HQS (h) PnPI-FBS (i) (j)

Figure 1: Results by different methods when recovering the image '0037' from kernel 2 and Gaussian noise with $\sigma = 12.75$. (a) Blurred. (b) MMO-FBS, PSNR=23.45dB. (c) NE-PGD, PSNR=23.59dB. (d) Prox-DRS, PSNR=23.53dB. (e) DPIR, PSNR=24.85dB. (f) PnPI-GD, PSNR=23.82dB. (g) PnPI-HQS, PSNR=25.16dB. (h) PnPI-FBS, PSNR=23.99dB. (i) PSNR curves, x-axis denotes iteration number. (j) Relative error curves, x-axis denotes iteration number.

In Fig. 1, we show deblurring results when recovering the image '0037' from kernel 2 and Gaussian noise $\sigma = 12.75$. It can be seen in Fig. 1 (a) that the image is severely blurred and noisy. Compared with MMO-FBS and NE-PGD,

Table 4: Average deblurring PSNR and SSIM performance by different methods on CBSD68 dataset with Levin's 8 kernels with $\sigma = 12.75$.

	kernel1	kernel2	kernel3	kernel4	kernel5	kernel6	kernel7	kernel8	Average
MMO-FBS	25.97	25.73	26.41	25.52	27.50	27.04	26.59	26.07	26.35
	0.6985	0.6871	0.7151	0.6723	0.7642	0.747	0.7282	0.7027	0.7100
NE-PGD	26.26	25.93	26.58	25.70	27.69	27.33	26.77	26.33	26.58
	0.7147	0.699	0.7252	0.6845	0.7749	0.7628	0.7413	0.7192	0.7277
Prox-DRS	26.30	25.92	26.50	25.87	27.81	26.92	27.23	26.56	26.64
	0.694	0.6829	0.7167	0.6807	0.7749	0.7451	0.7598	0.7215	0.7200
DPIR	27.43	27.21	27.61	26.98	28.57	28.34	27.75	27.29	27.65
	0.7649	0.755	0.7696	0.7434	0.8092	0.8018	0.7814	0.7651	0.7738
PnPI-GD	26.14	25.95	26.37	25.65	27.36	27.22	26.50	26.10	26.41
	0.6717	0.6729	0.7027	0.6581	0.7373	0.7240	0.7099	0.6932	0.6962
PnPI-HQS	**27.55**	**27.33**	**27.69**	**27.10**	**28.68**	**28.50**	**27.77**	**27.35**	**27.75**
	0.7719	**0.7641**	**0.7762**	**0.7531**	**0.8142**	**0.8091**	**0.7822**	**0.7668**	**0.7797**
PnPI-FBS	26.78	26.23	26.57	26.01	27.87	27.76	26.90	26.54	26.83
	0.7376	0.7170	0.7329	0.7042	0.7889	0.7836	0.7583	0.7381	0.7451

Table 5: Average deblurring PSNR and SSIM performance by different methods on CBSD68 dataset with Levin's 8 kernels with $\sigma = 17.85$.

	kernel1	kernel2	kernel3	kernel4	kernel5	kernel6	kernel7	kernel8	Average
MMO-FBS	25.56	25.39	26.01	25.16	26.76	26.36	25.96	25.59	25.72
	0.6856	0.6764	0.7007	0.6625	0.7351	0.7216	0.7041	0.6873	0.7000
NE-PGD	25.67	25.39	26.03	25.17	26.89	26.56	26.09	25.72	25.94
	0.6859	0.6724	0.6994	0.6590	0.7400	0.7292	0.7099	0.6908	0.6983
Prox-DRS	25.85	25.62	26.31	25.34	27.13	25.90	25.61	26.14	25.99
	0.6926	0.6704	0.7131	0.6646	0.7361	0.6875	0.6773	0.6922	0.6900
DPIR	26.41	26.26	26.78	26.04	27.60	27.28	26.85	**26.42**	26.75
	0.7226	0.7122	0.7326	0.7000	0.7751	0.7631	0.7452	**0.7452**	0.7293
PnPI-GD	25.28	25.21	25.69	24.90	26.46	26.34	25.70	25.27	25.61
	0.6329	0.6404	0.6760	0.6254	0.7036	0.6887	0.6782	0.6609	0.6633
PnPI-HQS	**26.53**	**26.31**	**26.84**	**26.11**	**27.69**	**27.45**	**26.90**	26.33	**26.77**
	0.7302	**0.7209**	**0.7450**	**0.7159**	**0.7796**	**0.7710**	**0.7536**	0.7252	**0.7386**
PnPI-FBS	25.82	25.52	25.96	25.32	26.98	26.86	26.29	25.88	25.97
	0.6838	0.6819	0.7047	0.6701	0.7517	0.7425	0.7256	0.7045	0.7081

PnPI-GD and PnPI-FBS provide results with better structure recovery, see Figs. 1 (b) (c) (f) (h). Compared with Prox-DRS and DPIR, the result by PnPI-HQS has clearer details, see Figs. 1 (d) (e) (g). Note that DPIR has no convergence guarantee, while PnPI-GD, PnPI-HQS, and PnPI-FBS are shown convergent in Figs. 1 (i) (j).

5 Single image super-resolution

In Table 6, we provide quantitive comparisons for single image super-resolution. It can be seen that the proposed method shows 0.3dB and 0.13dB improvement in PSNR, compared with other convergent PnP methods and DPIR respectively.

Table 6: Average super-resolution PSNR and SSIM performance by different methods on CBSD68 dataset with different scales and noise levels.

scale	s=2			s=4		
σ	0	2.55	7.65	0	2.55	7.65
MMO-FBS	27.02	26.16	25.28	25.30	25.17	24.51
	0.7719	0.7142	0.6604	0.6692	0.6602	0.6285
NE-PGD	27.02	26.23	25.27	25.34	25.21	24.54
	0.7822	0.7197	0.6622	0.6719	0.6632	0.6311
Prox-DRS	30.26	26.63	25.57	25.49	25.23	24.48
	0.8874	0.7364	0.6805	0.7007	0.6716	0.6280
DPIR	29.95	27.06	25.77	25.82	25.42	24.68
	0.8677	**0.7615**	0.6993	0.7099	0.6808	0.6398
PnPI-GD	25.54	25.36	25.12	25.06	25.01	24.30
	0.7201	0.7028	0.6766	0.6838	0.6728	0.6280
PnPI-HQS	**30.38**	**27.09**	**25.93**	**25.83**	**25.47**	**24.76**
	0.8822	0.7602	**0.7012**	**0.7108**	**0.6878**	**0.6480**
PnPI-FBS	28.12	26.29	25.44	25.43	25.29	24.53
	0.8306	0.7357	0.6846	0.6877	0.6795	0.6380

In Fig. 2, we provide visual results on the image '0046' when $s = 2$ and $\sigma = 2.55$. In Figs. 2 (b) (c) (f) (h), compared with MMO-FBS and NE-PGD, the proposed PnPI-GD and PnPI-FBS provide sharper edges. PnPI-HQS has clearer structures than Prox-DRS, see Figs. 2 (d) and (g). Note that the result by DPIR seems have some ringing artifacts. We account this for the non-convergent behavior of DPIR shown in Figs. 2 (i) (j), while the proposed methods have stable and convergent PSNR and relative error curves.

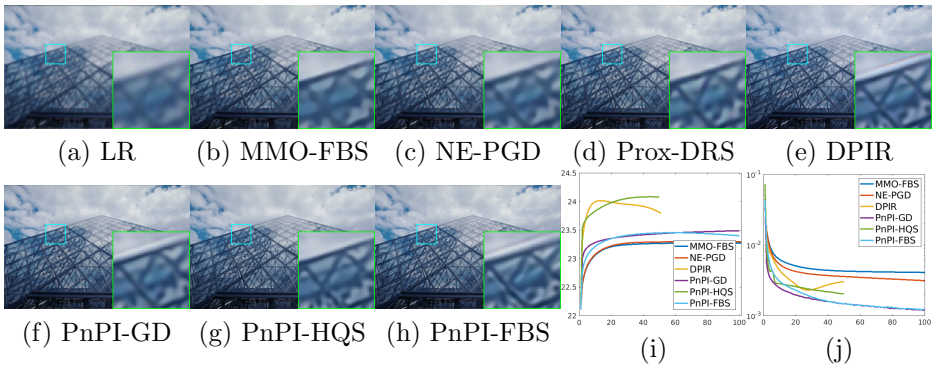

(a) LR (b) MMO-FBS (c) NE-PGD (d) Prox-DRS (e) DPIR

(f) PnPI-GD (g) PnPI-HQS (h) PnPI-FBS (i) (j)

Figure 2: Super-resolution results by different methods on the image '0046' from CBSD68 with $s = 2, \sigma = 2.55$. (a) Low-resolution (LR). (b) MMO-FBS, PSNR=23.28dB. (c) NE-PGD, PSNR=23.30dB. (d) Prox-DRS, PSNR=23.62dB. (e) DPIR, PSNR=23.80dB. (f) PnPI-GD, PSNR=23.50dB. (g) PnPI-HQS, PSNR=24.08dB. (h) PnPI-FBS, PSNR=23.38dB. (i) PSNR curves, x-axis denotes iteration number. (j) Relative error curves, x-axis denotes iteration number.